

# Relational Semantic Reasoning on 3D Scene Graphs for Open World Interactive Object Search

Imen Mahdi<sup>1</sup>, Matteo Cassinelli<sup>2</sup>, Fabien Despinoy<sup>2</sup>, Tim Welschehold<sup>1</sup>, Abhinav Valada<sup>1</sup>

<sup>1</sup>University of Freiburg    <sup>2</sup>Toyota Motor Europe

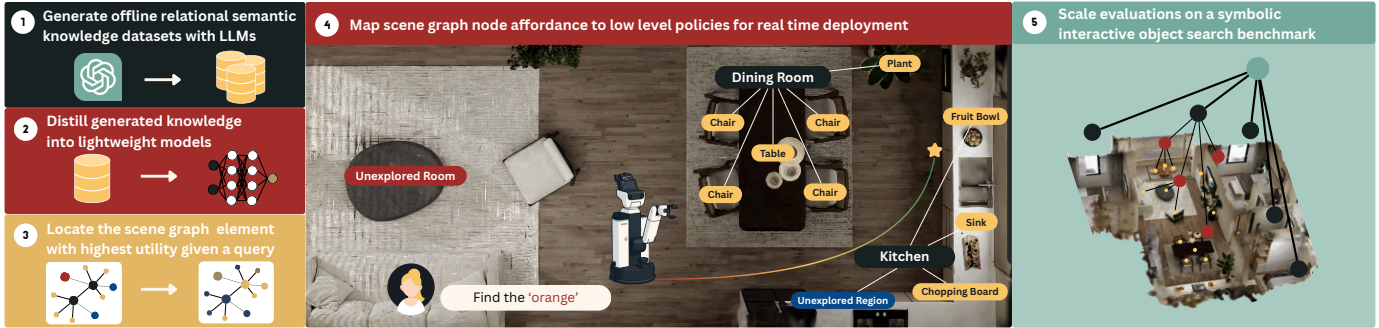


Fig. 1: **Overview of SCOUT: Scene Graph-Based Exploration with Learned Utility for Open-World Interactive Object Search.** SCOUT procedurally distills structured, relational semantic knowledge between scene elements from large language models into lightweight models (1–2). During exploration, the agent assigns utility scores to scene graph nodes based on exploration heuristics previously learned (3) and grounds high-level actions through low-level navigation and manipulation policies (4). SymSearch, our symbolic benchmark (5), enables scalable evaluation of relational semantic reasoning over scene graphs with no simulation overhead.

**Abstract**—Open-world interactive object search in household environments requires understanding semantic relationships between objects and their surrounding context to guide exploration efficiently. Prior methods either rely on vision–language embeddings similarity, which does not reliably capture task-relevant relational semantics, or large language models (LLMs), which are too slow and costly for real-time deployment. We introduce SCOUT: **SC**ene **G**raph-**B**ased **E**xploration with **L**earned **U**tility for **O**pen-**W**orld **I**nteractive **O**bject **S**earch, a novel method that searches directly over 3D scene graphs by assigning utility scores to rooms, frontiers, and objects using relational exploration heuristics such as room–object containment and object–object co-occurrence. To make this practical without sacrificing open-vocabulary generalization, we propose an offline procedural distillation framework that extracts structured relational knowledge from LLMs into lightweight models for on-robot inference. Furthermore, we present SymSearch, a scalable symbolic benchmark for evaluating semantic reasoning in interactive object search tasks. Extensive evaluations across symbolic and simulation environments show that SCOUT outperforms embedding similarity-based methods and matches LLM-level performance while remaining computationally efficient. Finally, real-world experiments demonstrate effective transfer to physical environments, enabling open-world interactive object search under realistic sensing and navigation constraints.

## I. INTRODUCTION

Robots operating in household environments must be able to search for objects efficiently, even when the target is hidden inside containers. Humans solve such tasks by leveraging rich semantic priors, such as what objects typically co-occur with and which rooms commonly contain them, which help guide the search without exhaustive exploration [16, 25]. Endowing robots with similar relational knowledge remains challenging,

especially in open-world settings where queries can reference arbitrary object categories.

Most existing object-search methods implicitly approximate these semantic priors using similarity between vision–language embeddings and a target query [10, 49, 5, 52]. While effective for measuring visual or functional similarity, such embeddings do not reliably encode relational semantics. For instance, “milk carton” may appear equally similar to “fridge” and “oven” in embedding space, despite only one being a plausible container. As a result, current embedding similarity-based search often struggles to distinguish semantically meaningful locations. This problem becomes more apparent when objects require interaction with the environment to be revealed, e.g. opening containers. Another class of methods [39, 46, 24, 48, 11, 51, 27, 7, 23, 6, 18, 28] relies on pretrained large language models (LLMs) to incorporate these semantic priors into their search pipelines implicitly. LLMs encode commonsense knowledge on human-centered environments and support open-vocabulary queries. However, online planning with LLMs is computationally expensive and unrealistic for autonomous agents with hardware constraints, as repeated queries scale poorly with scene complexity [29]. Knowledge distillation approaches [15, 33] mitigate this but require complex data generation pipelines and long training times.

In parallel, 3D scene graphs (3DSGs) [4, 45, 41] have emerged as compact, semantically structured representations for scene understanding. Their hierarchical structure makes them well-suited for relational reasoning tasks. However, most existing approaches utilize them to ground LLM-based planners

[32, 23, 6, 18, 28, 24, 48], leaving open the question of how to efficiently exploit their embedded knowledge without incurring high inference-time costs.

In this work, we propose SCOUT: Scene Graph-Based Exploration with Learned Utility for Open-World Interactive Object Search, an interactive object-search method that performs reasoning directly at the scene graph level. SCOUT assigns utility scores to rooms, regions, objects, and containers with respect to a given query by leveraging two key exploration heuristics: room–object containment and object–object co-occurrence. These scores guide exploration toward the most promising scene elements without requiring computationally expensive online LLM calls. To efficiently estimate these utility scores, we introduce an offline procedural distillation framework that extracts structured relational semantic knowledge from LLMs and trains lightweight models to predict containment and co-occurrence priors over scene elements. These distilled models retain open-vocabulary generalization while enabling on-robot inference. Finally, we present SymSearch, a symbolic, scene-graph-based benchmark that evaluates open-vocabulary relational semantic reasoning without simulation overhead. SymSearch realistically simulates how an embodied agent incrementally discovers rooms, frontiers, and objects, enabling scalable evaluation of exploration strategies.

In summary, our main contributions are the following:

- 1) SCOUT, a heuristics-based exploration method operating directly on 3D scene graphs.
- 2) A procedural LLM distillation framework that captures open-vocabulary relational semantic knowledge for real-time inference.
- 3) SymSearch, a scalable symbolic benchmark for open-world interactive object search.
- 4) A quantitative analysis of embedding limitations and a comprehensive evaluation showing that SCOUT surpasses embedding-based baselines and approaches LLM-level reasoning at a fraction of the computational cost, with successful transfer to real-world robots.
- 5) We make the code publicly available at <https://scout.cs.uni-freiburg.de>.

## II. RELATED WORK

Object search, also referred to as object goal navigation, in unknown environments has been widely studied [38, 37]. While classical approaches typically assume a closed set of object categories, realistic object search requires handling open-vocabulary queries. Recent methods address this by leveraging vision–language embeddings to estimate the relevance of observed regions to a textual query, using similarity scores as search heuristics. Common strategies include constructing relevance or semantic maps to score frontiers [10, 49, 5, 52, 30] or learning semantic-driven navigation policies [10]. Nevertheless, embedding similarity often yields noisy or ambiguous signals.

Alternatively, large language models have recently been adopted in robotic planning tasks due to their ability to reason over long horizons, handle open-vocabulary queries, and encode commonsense knowledge [9]. Among these methods [39, 46]

use them to score frontiers and spatial regions. However, these approaches assume that the target object can be observed without interaction. A central challenge in interactive exploration with LLMs is grounding reasoning in the physical world. Many approaches rely on 3D scene graphs [4] as compact and semantically rich representations that can be easily presented in textual format and constrain LLM outputs to a predefined set of high-level actions with arguments grounded in scene graph elements [32, 7, 23, 6, 28].

Several recent works apply LLMs and 3DSGs specifically to open-world object search by using them to select regions and objects to explore [24, 48] or to assign explicit relevance scores to candidate receptacles based on object and room categories [27]. MoMa-LLM [18] addresses interactive exploration by exposing a skill API that grounds abstract manipulation and exploration actions to elements of the 3DSG. To reduce LLM calls, GODHS [51] first exhaustively explores all rooms, then uses an LLM to rank rooms by their likelihood of containing the target object, and finally identifies and ranks receptacles within each room. Closer to our work is Seek [12] that trains relational semantic networks on small distilled data from LLMs and 3DSGs to guide exploration in industrial inspection tasks. We address interactive object search by explicitly incorporating search heuristics over scene graphs. We perform the search directly at the scene graph level by selecting the scene element with the highest utility to explore and mapping it to low-level policies via node affordances. To estimate utility in an open-vocabulary setting, we procedurally extract large relational semantic knowledge offline using LLMs and construct supervised datasets to train lightweight models suitable for real-time deployment.

Existing object search benchmarks [36, 42, 47, 50] primarily evaluate perception and navigation, providing limited support for semantic reasoning or interactive environments. Existing interactive simulators include AI2-THOR [21], which spans one-room scenes, and OmniGibson [22], which is computationally expensive and often unstable for generating scenes. Taskography [2] is a symbolic planning benchmark that enables fast evaluation using scene graphs but focuses on simple rearrangement tasks and does not evaluate semantic reasoning. In contrast, we propose a new symbolic benchmark designed to scale semantic reasoning evaluation over large, open-vocabulary 3D scene graphs that more closely resemble real household environments and offer substantially greater semantic diversity and scene complexity.

## III. PROBLEM FORMULATION

We study *open-world interactive object search* in unknown household environments. The agent receives an open-vocabulary language query  $q$  describing a target object and must locate it by actively exploring the scene (e.g., opening cabinets or doors) as target objects may be occluded within closed containers. At each timestep  $t$ , the agent constructs an incremental 3DSG  $\mathcal{G}_t$  from raw observations, such as egocentric RGB-D images  $\mathcal{I}_t$  and pose estimates  $P_t$  obtained from onboard odometry. Following [4], we define a hierarchical 3DSG as a directed tree  $\mathcal{G} = (\mathcal{V}, \mathcal{E})$ , with  $\mathcal{V}$  nodes,  $\mathcal{E}$

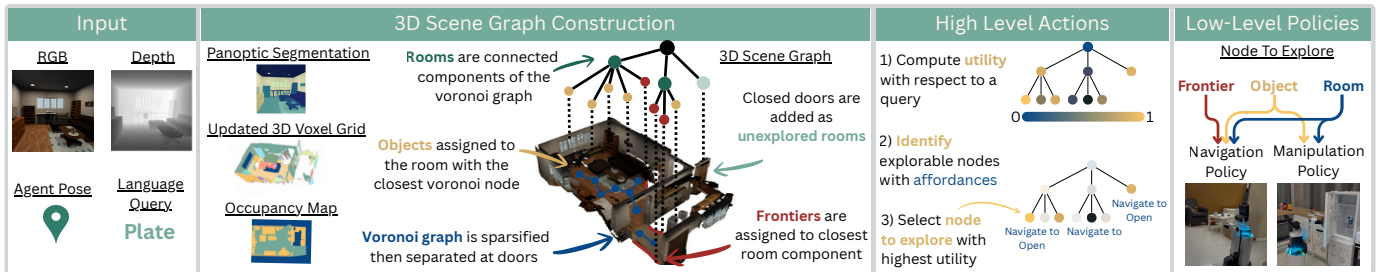


Fig. 2: **Full pipeline of SCOUT illustrated.** From left to right: 3DSG is constructed online from raw observations. Scene graph nodes are scored based on their utility in finding the query. Once the node to explore is selected, its affordances determine which low-level policies to run.

edges, and  $L$  layers of abstraction. Nodes represent scene elements such as rooms, regions, objects, or nested objects. Edges include inter-layer relations, e.g., rooms contain regions, regions contain objects, and intra-layer relations, e.g., rooms connected via doors. Each node has a unique parent in the preceding layer. Nodes carry open sets of attributes such as labels, positions, states, and affordances. We assume that the 3DSG construction can be performed by any of the existing methods [35, 19, 45, 13, 26]. In this setup, we distinguish between two levels of actions: high-level and low-level actions. High-level actions correspond to node-level affordances, e.g. navigate to and open an object, which are then executed through low-level navigation or manipulation policies. The task is considered solved when the target becomes visible, and the agent reaches it within a predefined distance threshold. In this work, we use a 5-layer hierarchy: *root*, *rooms*, *regions/frontiers*, *objects/containers*, and *nested objects*. Our goal is to leverage this structured representation to guide interactive search under open-vocabulary queries.

#### IV. SCOUT: SCENE GRAPH-BASED EXPLORATION WITH LEARNED UTILITY

We introduce SCOUT, a method that leverages the semantically rich scene graph structure, estimates the utility of observed scene elements to locate a given open-vocabulary query, and maps high-level actions to low-level policies accordingly. We first describe how 3DSGs are constructed from raw observations. We then define utility and describe how it is computed using exploration heuristics, and detail how these heuristics are learned via offline structured relational semantic knowledge distillation from LLMs. Finally, we detail how node-level actions are grounded by mapping affordances to low-level policies. The full pipeline is illustrated in Fig. 2.

##### A. 3DSG Construction

Real-world environments provide fine-grained observations and require the execution of low-level actions. Following the approach of Honerkamp et al. [18], Mohammadi et al. [28], we construct the 3DSG from RGB-D observations and pose estimates. We perform semantic and instance segmentation on the RGB images and fuse the results into a semantic voxel map using depth and pose information. This voxel map is then projected into a bird’s-eye-view (BEV) semantic map and an occupancy map. Similar to Hydra [19], we build a Voronoi-based navigation graph from the occupancy map. To identify

rooms, we sparsify the navigation graph and remove edges that intersect detected doors, resulting in connected components that correspond to individual room segments. Object instances extracted from the semantic voxel map are assigned to rooms by selecting the component associated with the nearest Voronoi node, and room categories are inferred from the objects they contain. Frontiers are extracted from the BEV occupancy map as boundaries between explored traversable space and unexplored regions [43]. Additionally, detected closed doors are treated as entrances to unexplored rooms and are added as nodes in the graph.

##### B. Estimating Utility via Exploration Heuristics

In interactive object search, relational semantics between the target query and elements observed in the scene provide informative cues for deciding where to explore next. Prior work often relies on vision–language embedding similarity to identify promising regions [10, 49, 5, 52]. However, embeddings typically capture visual or functional similarity, which is not always the most informative signal for exploration. Indoor objects exhibit strong contextual regularities: many objects co-occur with others, e.g., forks with plates and dishwashers, and follow a probability distribution over room categories, e.g., forks appearing predominantly in kitchens or dining rooms. These relational priors between a query and observed scene elements provide stronger cues for object search than visual similarity alone. Accordingly, we define a utility scoring function:

$$u_q(n) \in [0, 1], \quad (1)$$

which captures how informative a scene-graph node  $n$  is for localizing the queried object  $q$ . Motivated by human-inspired search heuristics, we approximate utility using object–object co-occurrence and room–object containment probabilities. This utility score is assigned differently based on the node type:

a) *Rooms*: If a room  $r$  is observed and categorized, its utility is given by

$$u_q(r) \approx p_{\text{contains}}(r, q), \quad (2)$$

where  $p_{\text{contains}}(r, q)$  is the probability that  $r$  contains the target object  $q$ . Unobserved rooms, e.g., detected from closed doors, are unclassified and therefore cannot be scored. To ensure they remain selectable when all visible nodes are uninformative, we assign them a default exploration score.

b) *Objects and Containers*: Objects’ utility is estimated through co-occurrence probabilities:

$$u_q(o) \approx p_{\text{co-occur}}(o, q), \quad (3)$$

where  $p_{\text{co-occur}}(o, q)$  denotes the probability that object  $o$  co-occurs with target object  $q$ . Because an object’s utility depends strongly on the room context (e.g., “kitchen cabinet” vs. “bathroom cabinet”), we update object scores as follows:

$$u_q^{\text{updated}}(o) = u_q(r_o) (w + (1 - w) u_q(o)), \quad (4)$$

where  $r_o$  is the parent room of object  $o$  and  $w \in [0, 1]$  controls how much influence the room has on the final score.

c) *Frontiers*: Each frontier is assigned an aggregated score based on nearby objects within a spatial radius. If no informative objects are nearby, e.g., a hallway frontier, we assign a default frontier exploration score to encourage expanding to unknown space.

### C. Learning Relational Semantics via Structured Knowledge Distillation

Relational semantic priors, such as co-occurrence or containment, are challenging to define for an open-set vocabulary. Typically, these heuristics are implicitly obtained through online LLM planning. Instead, we extract them offline via structured querying of a pretrained LLM and distill this knowledge into lightweight supervised models that retain open-vocabulary generalization. Specifically, our goal is to construct a supervised learning dataset given a semantic relation, e.g., co-occurrence or containment, by procedurally querying an LLM

$$\mathcal{D}_{\text{relation}} = \{(x_i, y_i)\}_{i=1}^N,$$

where  $x_i$  denotes a pair of textual inputs and  $y_i$  is the corresponding utility score. A key challenge in generating a large, diverse set of object categories with LLMs is encountering hallucinations or token limits. Instead, we procedurally prompt the LLM to construct our initial set of open vocabulary object categories  $\mathcal{O}_{\text{household}}$ . To do so, the LLM first generates a set of rooms  $\mathcal{R}$ , the object categories  $\mathcal{C}(r)$  associated with each room  $r$ , and the set of objects for each room–category pair  $\mathcal{O}(r, c)$ . This yields

$$\mathcal{O}_{\text{household}} = \bigcup_{r \in \mathcal{R}} \bigcup_{c \in \mathcal{C}(r)} \mathcal{O}(r, c). \quad (5)$$

We then use this initial set to generate two relational datasets. For object–object co-occurrence, the LLM proposes, for each query  $q \in \mathcal{O}_{\text{household}}$ , a set of objects annotated with binary co-occurrence labels, i.e., 1 if the object is likely to co-occur with the target query and 0 otherwise. For room–object containment, the LLM provides a list of rooms with continuous scores  $y \in [0, 1]$ , i.e., the probability that an object  $q$  is found in room  $r$ . For object co-occurrence, we experimented with both binary and continuous labels and found that continuous scores are better suited for this task. We attribute this to the inherent ambiguity of object–object relationships, which are often difficult to quantify precisely (e.g., how much more likely a pen is to co-occur with a desk than with paper). In

contrast, room–object associations are more structured and can be meaningfully expressed as continuous probabilities (e.g., a cup’s most probable room locations might be: kitchen, living room, bedroom, bathroom, in decreasing order). The final datasets obtained are thus:

$$\mathcal{D}_{\text{co-occur}} = \{((o, q)_i, y_i)\}_{i=1}^N, \quad (6)$$

and

$$\mathcal{D}_{\text{contain}} = \{((r, q)_i, y_i)\}_{i=1}^M, \quad (7)$$

with  $N$  and  $M$  denoting the sizes of each dataset, respectively.

Once the datasets are constructed, they serve as ground truth to train our lightweight models. To ensure generalization, we first embed textual input using a frozen pretrained text encoder  $E$  and concatenate embeddings to form inputs  $x \in \mathbb{R}^{2d}$  with  $d$  being the embedding dimension. A simple parametric model

$$f_{\theta}^{\text{relation}} : \mathbb{R}^{2d} \rightarrow [0, 1] \quad (8)$$

is then learned via supervised learning.

Concretely, we train two MLPs:  $f_{\theta_1}^{\text{co-occur}}$  with binary cross entropy as loss function and  $f_{\theta_2}^{\text{contain}}$  with mean squared error as loss function. This distillation procedure ensures (i) low inference costs during online exploration and (ii) generalization to an open vocabulary set of objects and query descriptions that come from the pretrained embeddings.

Finally, these models define the utility scoring functions used to score scene graph nodes following Eq 2 and 3:

$$u_q(o) = f_{\theta_1}^{\text{co-occur}}(E(o) \oplus E(q)), \quad (9)$$

$$u_q(r) = f_{\theta_2}^{\text{contain}}(E(r) \oplus E(q)), \quad (10)$$

where  $\oplus$  denotes dimension-wise concatenation.

### D. Selecting and Grounding High Level Actions

After all nodes are scored, the agent considers the set of actionable nodes  $\mathcal{N}_a$ , i.e., nodes with exploration affordances such as openable containers, closed doors, or unexplored frontiers. To avoid excessive travel, distance is incorporated into the selection. Specifically, let  $U_{\text{max}}$  denote the maximum utility scored among actionable nodes. The agent first selects nodes with a utility score in the range  $[U_{\text{max}} - \Delta, U_{\text{max}}]$ , where  $\Delta$  is a pre-defined margin that ensures elements with close scores are equally important, and then chooses the one with minimum travel distance:

$$n^* = \arg \min_{n \in \mathcal{N}'_a} d(n), \quad (11)$$

where  $\mathcal{N}'_a = \{n \in \mathcal{N}_a \mid u_q(n) \geq U_{\text{max}} - \Delta\}$ , and  $d(n)$  is the estimated geodesic distance from the current robot position to the target node  $n$ . Note that setting  $\Delta = 0$  is the same as taking the highest scoring node at each timestep greedily:

$$n^* = \arg \max_{n \in \mathcal{N}_a} u_q(n). \quad (12)$$

Once a scene-graph node  $n^*$  is selected for exploration, its affordance dictates the subsequent action and low-level policy. For navigable nodes, e.g., frontiers or objects, the agent plans

a collision-free path to the nearest Voronoi node using A\* on an inflated occupancy map. If a selected object is openable, the agent invokes a manipulation policy to open it. In practice, the agent first navigates to the target; if the target is a container, i.e., has an “openable” affordance, the agent then transitions to the manipulation policy to explore its contents.

## V. SYMBOLIC OBJECT SEARCH ON 3D SCENE GRAPHS

We propose a flexible symbolic benchmark for interactive object search that satisfies the following requirements:

- **Scene-graph based representation:** uses 3D Scene Graphs, enabling compatibility with any dataset source and supporting arbitrary hierarchical depths, node attributes, and edge types.
- **Open-vocabulary semantics:** supports open set object and room categories and attributes.
- **Exploration realism:** mimics how an embodied agent perceives and incrementally explores an environment.
- **Evaluation of semantic reasoning:** Focuses on evaluating high-level decision-making based on semantics.

### A. 3D Scene-Graph Construction from Real Indoor Scans

In this environment, a scene is represented as a hierarchical 3DSG  $\mathcal{G}$  described in Sec III. To this end, we consider InteriorGS [40], a Gaussian-splatting dataset of 1,000 human-centric indoor scenes (e.g., homes, restaurants, beauty salons) with dense object annotations. Each scene includes a Gaussian splat of the full environment, object bounding boxes with semantic labels, room and door polygons, and a top-down occupancy map. We extract 3DSG representations tailored to our environment as follows: **Objects:** Each annotated object instance includes a semantic class and a 3D bounding box. We take the bounding-box center as the node position and the semantic label as the object category. **Rooms:** Room polygons are used to assign objects to rooms. Room classification is inferred via an LLM conditioned on room contents and manually refined to ensure accuracy. Door bounding boxes are used to derive room connectivity by detecting intersections between rooms and door polygons. **Regions:** For each room, we cluster object positions  $(x, y)$  using a Gaussian Mixture Model (GMM). The number of components is selected via the Bayesian Information Criterion (BIC) within predefined bounds. These clusters approximate spatially coherent regions that an agent would reveal during exploration. **Nested Objects:** For object-object relations, we manually annotate *on-top-of* and *inside* edges using the underlying Gaussian splats, since bounding boxes alone produce unreliable relationships.

Furthermore, we use the occupancy map of the scene  $M_{\mathcal{G}}$  to compute realistic traveled distances. To do so, we first sample the closest unoccupied point to the goal object within the same room and compute the geodesic path using Dijkstra’s algorithm on the dilated occupancy map.

In Table I, we compare the diversity and complexity of InteriorGS with two existing interactive simulators, AI2-THOR [21] and OmniGibson [22]. AI2-THOR consists exclusively of single-room scenes. OmniGibson includes larger

scenes populated mostly with furniture and fixtures. Although additional objects can be sampled, doing so frequently results in failures and limits scalability. InteriorGS has a more diverse set of object categories, along with more fine-grained and descriptive room annotations. During manual annotation, we also ensure that realistic and diverse object-object relations are maintained.

### B. Environment Roll-out

The roll-out process, illustrated in Fig. 3, simulates how an agent incrementally explores a scene. Each episode begins by spawning the agent in a random region within a random room. The agent is provided with a query object  $q$ , an observed subgraph  $\mathcal{G}_{\text{obs}}$  consisting of objects and rooms previously observed, frontier nodes, i.e., regions whose children are not yet revealed, and unexplored room nodes, i.e., rooms connected via doors but not yet visited with all attributes hidden.

Actions correspond to selecting a node to explore as follows:

- **Exploring an unexplored room:** reveals the closest region relative to the agent, all first-level objects in that region, and any additional connected frontiers or rooms.
- **Exploring a frontier:** reveals the first-level objects in the corresponding region.
- **Exploring an object:** reveals its nested objects (e.g., objects inside containers or supported by the object).

The episode terminates when the query object  $q$  becomes visible to the agent or when a maximum number of steps  $N_{\text{max}}$  is reached. An episode is successful if the agent reveals the goal object within  $N_{\text{max}}$  steps.

## VI. EXPERIMENTAL EVALUATION

Our experiments are designed to answer the following:

- Do our learned utility scoring functions improve search efficiency compared to embedding similarity?
- Can our method match the performance of online LLM-based planners with a fraction of the runtime?
- Does our method transfer to real-world applications?

### A. Implementation Details

As described in Sec IV-C, we procedurally generate two supervised learning datasets using `gpt-4o`. The generated data span  $N_{\text{objects}} = 3824$  unique object categories, with dataset sizes of 92K samples for containment and 7.5K samples for co-occurrence. Dataset generation required approximately three hours per dataset. We then use a frozen SBERT embedder to vectorize the inputs and train two 3-layer MLPs.

### B. Limitations of Embedding Similarity

Embeddings are widely used to compute similarity between a query and observations (e.g., a language query and RGB images), which are then used to guide downstream tasks such as object search. While effective in measuring visual or conceptual similarity, they fall short in encoding relational semantic information critical for reasoning and decision-making. To illustrate these limitations, we analyze the similarity distributions of different relational semantics using pretrained text-only embedders

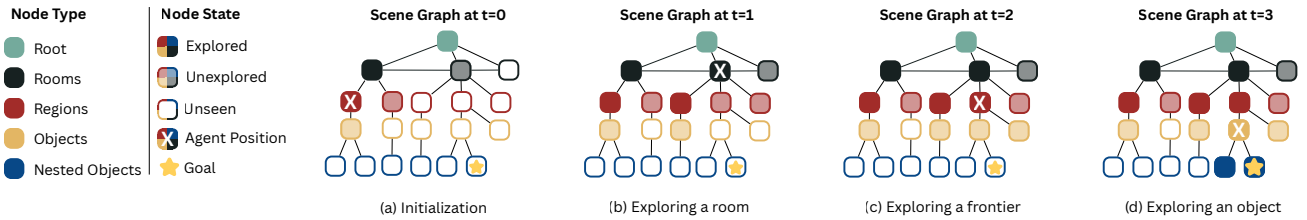


Fig. 3: **Illustration of SymSearch’s roll-out process.** At each step, the agent receives a scene-graph observation and a target object query. (a) At initialization, the agent spawns in a random region and room. Unexplored regions appear as frontier nodes, and rooms connected via doors are seen but unexplored. (b) Exploring a new room reveals the closest region to the agent in that room, along with its objects. The remaining regions are considered unexplored frontiers. (c) Exploring a frontier reveals the objects within that region. (d) Exploring an object reveals its nested objects (e.g., objects inside or on top of it). The episode terminates when the target object becomes visible.

TABLE I: **Statistics on interactive benchmarks.** We report dataset scale, semantic diversity, and scene complexity.

Benchmark	Scenes	Room Cat.	Obj. Cat.	Rooms/Sc.	Room Cat./Sc.	Obj./Sc.	Obj. Inst./Sc.	Contained Obj./Sc.
AI2-THOR	120	4	117	1.0	1.0	46.3	30.6	17.9
OmniGibson	45	39	237	7.1	<b>5.3</b>	245.0	31.4	6.3
InteriorGS	<b>1000</b>	<b>687</b>	<b>697</b>	<b>6.6</b>	5.1	<b>408.3</b>	<b>52.4</b>	<b>157.5</b> *

\* Average computed only over scenes that have been annotated so far.

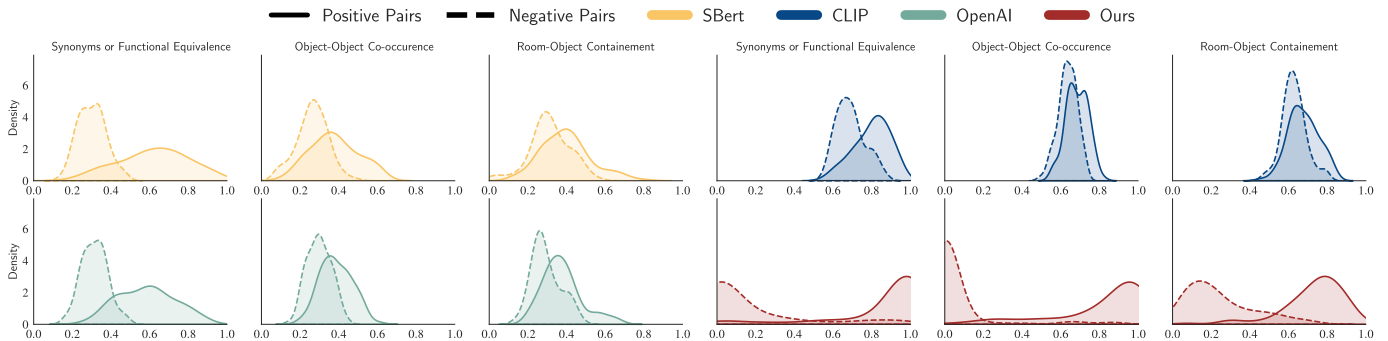


Fig. 4: **Comparison of embedding similarity distributions with our learned relational scoring models.** Synonym pairs are separable across all models, whereas co-occurrence and containment relationships are not. Our learned models produce substantially stronger separation.

including SBert [34] and OpenAI vector embeddings as well as a vision–language embedder CLIP [31], and compare them with our learned scoring functions  $f_{\theta_1}^{co-occur}$  and  $f_{\theta_2}^{contain}$ . We consider three categories: (a) synonyms or functionally equivalent objects, (b) object–object co-occurrence, and (c) room–object containment. Each category includes positive pairs (e.g., mug–cup, sofa–television, kitchen–oven) and negative pairs (e.g., chair–table, plate–shampoo, fridge–bedroom) respectively. Figure 4 shows the similarity and our learned scores distributions across these categories. While synonyms (a) are generally well separated, the distributions for co-occurrence (b) and room–object containment (c) show significant overlap between positive and negative pairs. This indicates that current embedding similarity-based methods lack the discriminative power to encode relational semantics. In contrast, our learned relevance models, which are explicitly trained on co-occurrence and containment relations, produce clearly separated distributions.

### C. Experimental Setup

We evaluate our approach on two environments:

**Symbolic Benchmark:** We evaluate in our SymSearch benchmark over 200 episodes across 10 indoor household scenes from the InteriorGS dataset, using 142 unique open-vocabulary

object queries, including 61 categories that do not exist in the training data used in Sec VI-A. Among these, 115 target objects are not immediately observable and require interaction with other objects to be discovered. We set the maximum episode length to  $N_{\max} = 50$  steps.

**Simulation Benchmark:** We extend the OmniGibson simulator with an interactive object search task definition. Target objects are spawned using the simulator’s internal object sampler, either inside containers or within rooms. For each episode, a goal object is sampled in a specified room or placed inside/on top of another object. We generate 50 episodes with 50 unique BEHAVIOR-1K objects across 11 scenes. Among these, 27 objects are not included in the training data, and 25 require interactivity. To fairly evaluate semantic reasoning performance between baselines, the agent uses an oracle “magic open” manipulation action and ground truth segmentation to avoid failure cases caused by manipulation or perception. We set  $N_{\max} = 35$  steps.

As metrics, we compute the Success Rate (SR) and Success weighted by Path Length (SPL). Additionally, we record the number of high-level steps taken per episode and the average inference time to quantify exploration efficiency.

We compare our agent against the following baselines:

TABLE II: **Evaluation results on SymSearch and Omnigibson.** Table reports the success rate percentage, SPL, average number of steps (high-level actions) per episode, and average inference time in seconds. Results on SymSearch are averaged across 5 different seeds. We report the **best**, **second-best**, and **third-best** results for each metric, respectively.

Method	Agent	SymSearch				Omnigibson			
		SR $\uparrow$	SPL $\uparrow$	N Steps $\downarrow$	Inference Time (s) $\downarrow$	SR $\uparrow$	SPL $\uparrow$	N Steps $\downarrow$	Inference Time (s) $\downarrow$
Random	Random Agent	0.337 $\pm$ 0.033	0.072 $\pm$ 0.010	47 $\pm$ 2	8 $\pm$ 0	-	-	-	-
Embedding Similarity	CLIP Similarity	0.638 $\pm$ 0.013	0.171 $\pm$ 0.020	34 $\pm$ 1	12 $\pm$ 0	0.565	0.322	23	15
	SBERT Similarity	0.683 $\pm$ 0.019	0.179 $\pm$ 0.024	33 $\pm$ 1	8 $\pm$ 0	0.632	0.241	24	1
LLM-based	MoMa-LLM [18]	0.827 $\pm$ 0.012	0.256 $\pm$ 0.020	20 $\pm$ 1	295 $\pm$ 21	0.696	0.257	17	300
	GODHS [51]	0.906 $\pm$ 0.011	0.161 $\pm$ 0.016	20 $\pm$ 0	39 $\pm$ 2	0.478	0.087	26	35
Ours	SCOUT (no room influence, $\Delta = 0$ )	0.817 $\pm$ 0.004	0.234 $\pm$ 0.013	23 $\pm$ 1	6 $\pm$ 0	0.745	0.340	23	1
	SCOUT (no room influence)	0.815 $\pm$ 0.012	0.269 $\pm$ 0.018	24 $\pm$ 0	6 $\pm$ 0	0.756	0.336	23	1
	SCOUT ( $\Delta = 0$ )	0.845 $\pm$ 0.004	0.220 $\pm$ 0.017	21 $\pm$ 0	6 $\pm$ 0	0.826	0.413	18	1
	SCOUT	0.846 $\pm$ 0.013	0.271 $\pm$ 0.022	22 $\pm$ 0	6 $\pm$ 0	0.829	0.415	19	1

- **Random agent:** uniformly samples actionable nodes.
- **Embedding-based agents:** Current baselines that use embedding similarity to guide the search do not support interactive exploration. We approximate them with an instance identical to our agent, except that utility is approximated using SBERT [34] or CLIP [31] similarity instead of the learned models. We tune the default room and frontier exploration scores to account for the distributional shift.
- **MoMa-LLM [18]:** queries an LLM at every high-level decision step to select the next action.
- **GODHS [51]:** first exhaustively explores all rooms, then uses an LLM to rank rooms by query relevance and to enumerate potential carrier objects within each room.

Consistent with existing literature [32, 18, 28], we found that the OpenAI GPT later series [1] performs best for reasoning and planning tasks. We opted for the "gpt-5 mini" model for both agents due to its ability to handle structured output and offer a compromise between performance and cost. Comparative results across different LLMs, including open-source alternatives, are provided in the supplementary material.

Finally, we evaluate model ablations, including disabling room-based score updates and setting  $\Delta = 0$ . We provide more implementation details and hyperparameters used to instantiate our agent in the supplementary material.

#### D. Evaluation Results

Table II summarizes results on both benchmarks. On the symbolic benchmark, embedding-based baselines outperform the random agent but remain well below stronger methods. GODHS achieves a high SR but a low SPL due to an exhaustive exploration phase. MoMa-LLM attains competitive SPL but relies on costly LLM calls at every step, leading to inference costs two orders of magnitude higher. Our method consistently outperforms embedding-based agents in both SR and SPL, while matching LLM-based SR at a fraction of the computational cost. Ablations show that room influence has the largest impact on SR, while removing the utility margin reduces efficiency, as the agent greedily selects high-scoring nodes without accounting for traveled distance.

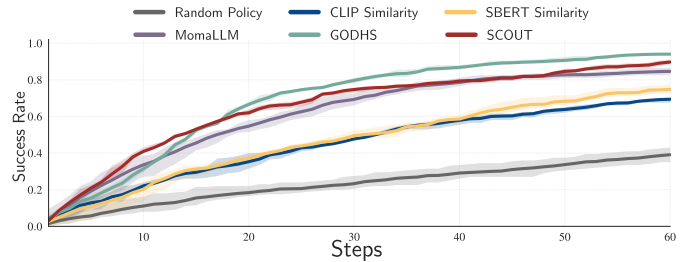


Fig. 5: **Success rate over an increasing number of steps on SymSearch.** Our method closely follows the performance of LLM-based baselines throughout the roll-out.

Figure 5 shows the success rate over an increasing number of steps. Throughout the roll-out, our agent closely matches and often surpasses LLM-based planners, particularly in early stages, where it effectively balances exploration and exploitation. In contrast, GODHS initially over-explores rooms, while MoMa-LLM exhibits higher variance and slightly lower SR due to non-determinism and hallucinations.

Contrary to SymSearch where agents have privileged information of when all rooms have been explored, the simulation benchmark poses more challenges that can arise from the real-time scene exploration and scene graph construction. This means that an efficient strategy must balance exploration and exploitation. As a result, GODHS performance drops as it over-explores all frontiers and closed doors. MoMa-LLM performs slightly better but also tends to prefer exploring unexplored space over attempting to open objects. In both evaluations, our agent balanced exploration and exploitation for maximum efficiency, surpassing the performance of LLM-based planners while remaining up to two orders of magnitude faster at inference.

#### E. Real-World Robot Experiments

To evaluate the real-world applicability of our method, we deploy it on a mobile manipulator (Toyota HSR) operating in a multi-room apartment environment with a kitchen, office, and living room. Given only a textual object query, the robot must locate the object using only the onboard RGB-D camera and localization as inputs. We follow the same pipeline described



Fig. 6: **Real-world robot experiments.** The robot’s high-level-actions are grounded to the scene through object affordances. The robot can open containers to locate potential target objects (e.g., fridge, drawer, cabinet) or explore on top of furniture (e.g., table, desk, counter).

in Sec IV-A. Additionally, we use the YOLO-World [8] model for real-time open-vocabulary semantic segmentation, and we add the target object to the list of labels at initialization. To efficiently evaluate reasoning, manipulation actions, i.e., opening containers, are executed using N2M2 [17] with pre-recorded opening motions defined relative to AR markers. More precisely, the robot first navigates to the Voronoi node closest to the object’s estimated location. Then, if the associated AR marker is observed, the corresponding N2M2 motion is executed. To this end, we provide a list of affordances for object labels that can be opened or explored (i.e., the robot navigates to the object and examines it).

We conduct 36 real-robot experiments across 12 distinct query object categories, with 7 objects placed inside containers (e.g., fridges or drawers). In all trials, the agent starts from a random location in the environment. We detail the experimental setup and provide examples in the supplementary material. We deem a trial successful if the agent locates the target object while efficiently prioritizing relevant rooms and avoiding unnecessary exploration. We categorize failures into three modes based on their root cause: perception, manipulation, and reasoning. Perception failures include missing the target object or misclassifying objects, which can affect room classification. Manipulation failures occur when the agent attempts to interact with a container but does not fully or correctly execute the action (e.g., partially opening a fridge and failing to reveal the target). Reasoning failures are caused by our method itself, such as assigning an incorrectly high utility score to an irrelevant room or container, or underestimating a plausible placement.

Figure 7 shows the distribution of successful and failed trials, along with the relative frequency of each failure mode. Overall, we achieve a 64% success rate, including interactive scenarios. For example, when searching for a book, if the robot identifies cabinets in both the kitchen and the living room, it avoids opening kitchen cabinets, reflecting common-sense reasoning about object placement. The primary bottleneck is the accuracy of the perception system. Our method relies on a faithful scene graph to operate efficiently; segmentation errors such as duplicated object instances or hallucinated objects can corrupt room classification and mislead the search. In some cases, the robot repeatedly attempts to open visually identical drawers or cabinets that are redundantly represented in the graph, or fails entirely if the target object is not detected. From these real-robot experiments, we draw two main conclusions. First, we evaluate the reasoning capabilities of our model under realistic system noise and demonstrate that it reproduces common-

TABLE III: **Runtime breakdown per timestep.** Average execution time (in seconds) for each component of the pipeline.

Scene Graph Construction	Inference (Node Selection)	Execution (Nav. + Manip.)	Total
$5.036 \pm 0.016$	$0.211 \pm 0.095$	$34.348 \pm 24.810$	$39.596 \pm 24.807$

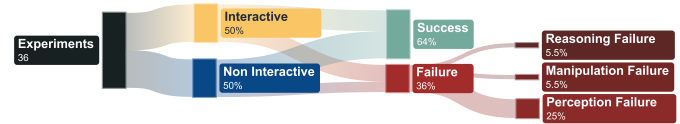


Fig. 7: **Distribution of real-robot experiments.** We conduct a total of 36 experiments, of which 50% require interactivity with the environment (i.e., the target object is hidden inside containers). Failure modes are primarily due to errors in the perception system.

sense behaviors distilled from an LLM. Second, we show that our approach can reason over 3D scene graphs, ground this reasoning in the physical world, and extend it to interactive search by mapping object affordances to low-level control policies. In Table III, we report a breakdown of the per-timestep runtime into three components: scene graph construction, inference time (selecting the next node to explore), and execution time (low-level policy execution, including navigation and control inference). Our method can run efficiently on a real robot without incurring major inference time costs.

#### F. Discussion and Limitations

We demonstrate that our method can: (1) generalize to an open set of object categories across scenes and benchmarks. (2) efficiently leverage the common-sense knowledge in LLMs while maintaining fast runtime inference time by exploiting exploration heuristic and our proposed procedural distillation framework. (3) match and surpass an LLM-planner performance at a fraction of the computational cost. (4) effectively transfer to realistic household settings. Despite these strengths, real-robot experiments reveal limitations. Performance depends heavily on the quality of the generated 3D scene graph and the reliability of real-time perception. Errors in object detection, localization, or room classification can lead to suboptimal or inefficient exploration. Moreover, our method encodes typical object–room relationships and implicitly assumes similar household structures. It does not currently model household- or user-specific object placement preferences, which may limit robustness in diverse real-world environments.

## VII. CONCLUSION

We introduced SCOUT (Scene Graph-Based Exploration with Learned Utility for Open-World Interactive Object Search), a method for interactive object search that leverages the semantic structure of scene graphs and human-inspired search heuristics. Our results demonstrate that lightweight relational semantic models distilled from LLM knowledge can effectively guide exploration. We demonstrate that SCOUT outperforms embedding-based heuristics and matches or exceeds LLM-based planners at a fraction of the computational cost. We further validate the practicality of our approach through successful deployment on a mobile manipulator in a real

household environment. Future work will address both adapting the learned utility scores to specific households by integrating observations on the fly and generalizing the method to more diverse human-centered environments.

#### ACKNOWLEDGMENTS

This work was funded by Toyota Motor Europe.

#### REFERENCES

- [1] Josh Achiam, Steven Adler, Sandhini Agarwal, Lama Ahmad, Ilge Akkaya, Florencia Leoni Aleman, Diogo Almeida, Janko Altenschmidt, Sam Altman, Shyamal Anadkat, et al. Gpt-4 technical report. *arXiv preprint arXiv:2303.08774*, 2023.
- [2] Christopher Agia, Krishna Murthy Jatavallabhula, Mohamed Khodeir, Ondrej Miksik, Vibhav Vineet, Mustafa Mukadam, Liam Paull, and Florian Shkurti. Taskography: Evaluating robot task planning over large 3d scene graphs. In *Conference on Robot Learning*, pages 46–58, 2022.
- [3] AI Anthropic. The claude 3 model family: Opus, sonnet, haiku. *Claude-3 Model Card*, 1(1):4, 2024.
- [4] Iro Armeni, Zhi-Yang He, JunYoung Gwak, Amir R Zamir, Martin Fischer, Jitendra Malik, and Silvio Savarese. 3d scene graph: A structure for unified semantics, 3d space, and camera. In *Proc. of the Int. Conf. Comput. Vis.*, 2019.
- [5] Utkarsh Bajpai, Julius Rückin, Cyrill Stachniss, and Marija Popović. Uncertainty-informed active perception for open vocabulary object goal navigation. *arXiv preprint arXiv:2506.13367*, 2025.
- [6] Meghan Booker, Grayson Byrd, Bethany Kemp, Aurora Schmidt, and Corban Rivera. Embodiedrag: Dynamic 3d scene graph retrieval for efficient and scalable robot task planning. *arXiv preprint arXiv:2410.23968*, 2024.
- [7] Georgia Chalvatzaki, Ali Younes, Daljeet Nandha, An Thai Le, Leonardo FR Ribeiro, and Iryna Gurevych. Learning to reason over scene graphs: a case study of finetuning gpt-2 into a robot language model for grounded task planning. *Frontiers in Robotics and AI*, 10:1221739, 2023.
- [8] Tianheng Cheng, Lin Song, Yixiao Ge, Wenyu Liu, Xinggang Wang, and Ying Shan. Yolo-world: Real-time open-vocabulary object detection. In *Proceedings of the IEEE/CVF conference on computer vision and pattern recognition*, pages 16901–16911, 2024.
- [9] Eugenio Chisari, Jan Ole Von Hartz, Fabien Despinoy, and Abhinav Valada. Robotic task ambiguity resolution via natural language interaction. In *IEEE/RSJ International Conference on Intelligent Robots and Systems (IROS)*, pages 14821–14827, 2025.
- [10] Samir Yitzhak Gadre, Mitchell Wortsman, Gabriel Ilharco, Ludwig Schmidt, and Shuran Song. Cows on pasture: Baselines and benchmarks for language-driven zero-shot object navigation. In *Proc. of the IEEE Conf. Computer Vision Pattern Recognition*, pages 23171–23181, 2023.
- [11] Wenqi Ge, Chao Tang, and Hong Zhang. Commonsense scene graph-based target localization for object search. In *Proc. of the IEEE/RSJ Int. Conf. on Intelligent Robots and Systems*, pages 13318–13325, 2024.
- [12] Muhammad Fadhil Ginting, Sung-Kyun Kim, David D Fan, Matteo Palieri, Mykel J Kochenderfer, and Ali-akbar Agha-Mohammadi. Seek: Semantic reasoning for object goal navigation in real world inspection tasks. *arXiv preprint arXiv:2405.09822*, 2024.
- [13] Qiao Gu, Ali Kuwajerwala, Sacha Morin, Krishna Murthy Jatavallabhula, Bipasha Sen, Aditya Agarwal, Corban Rivera, William Paul, Kirsty Ellis, Rama Chellappa, et al. Conceptgraphs: Open-vocabulary 3d scene graphs for perception and planning. In *Proc. of the IEEE Int. Conf. on Robotics and Automation*, pages 5021–5028, 2024.
- [14] Daya Guo, Dejian Yang, Haowei Zhang, Junxiao Song, Peiyi Wang, Qihao Zhu, Runxin Xu, Ruoyu Zhang, Shirong Ma, Xiao Bi, et al. Deepseek-r1 incentivizes reasoning in llms through reinforcement learning. *Nature*, 645(8081):633–638, 2025.
- [15] Huy Ha, Pete Florence, and Shuran Song. Scaling up and distilling down: Language-guided robot skill acquisition. In *Conference on Robot Learning*, pages 3766–3777, 2023.
- [16] Barbara Hidalgo-Sotelo, Aude Oliva, and Antonio Torralba. Human learning of contextual priors for object search: where does the time go? In *Proc. of the IEEE Conf. Computer Vision Pattern Recognition*, pages 86–86, 2005.
- [17] Daniel Honerkamp, Tim Welschehold, and Abhinav Valada. N2m2: Learning navigation for arbitrary mobile manipulation motions in unseen and dynamic environments. *IEEE Trans. on Robot.*, 39(5):3601–3619, 2023.
- [18] Daniel Honerkamp, Martin Büchner, Fabien Despinoy, Tim Welschehold, and Abhinav Valada. Language-grounded dynamic scene graphs for interactive object search with mobile manipulation. *IEEE Robotics and Automation Letters*, 2024.
- [19] Nathan Hughes, Yun Chang, and Luca Carlone. Hydra: A real-time spatial perception system for 3d scene graph construction and optimization. *arXiv preprint arXiv:2201.13360*, 2022.
- [20] Albert Qiaochu Jiang, Alexandre Sablayrolles, Arthur Mensch, Chris Bamford, Devendra Singh Chaplot, Diego de Las Casas, Florian Bressand, Gianna Lengyel, Guillaume Lample, Lucile Saulnier, L  lio Renard Lavaud, Marie-Anne Lachaux, Pierre Stock, Teven Le Scao, Thibaut Lavril, Thomas Wang, Timoth  e Lacroix, and William El Sayed. Mistral 7b. *arXiv preprint arXiv:2310.06825*, 2023.
- [21] Eric Kolve, Roozbeh Mottaghi, Winson Han, Eli Vander-Bilt, Luca Weihs, Alvaro Herrasti, Matt Deitke, Kiana Ehsani, Daniel Gordon, Yuke Zhu, et al. Ai2-thor: An interactive 3d environment for visual ai. *arXiv preprint arXiv:1712.05474*, 2017.
- [22] Chengshu Li, Ruohan Zhang, Josiah Wong, Cem Gokmen, Sanjana Srivastava, Roberto Mart  n-Mart  n, Chen Wang, Gabriel Levine, Wensi Ai, Benjamin Martinez, et al.

- Behavior-1k: A human-centered, embodied ai benchmark with 1,000 everyday activities and realistic simulation. *arXiv preprint arXiv:2403.09227*, 2024.
- [23] Yuchen Liu, Luigi Palmieri, Sebastian Koch, Ilche Georgievski, and Marco Aiello. Delta: Decomposed efficient long-term robot task planning using large language models. *arXiv preprint arXiv:2404.03275*, 2025.
- [24] Joel Loo, Zhanxin Wu, and David Hsu. Open scene graphs for open-world object-goal navigation. *The International Journal of Robotics Research*, 2025.
- [25] Stephen C Mack and Miguel P Eckstein. Object co-occurrence serves as a contextual cue to guide and facilitate visual search in a natural viewing environment. *Journal of vision*, 11(9):9–9, 2011.
- [26] Dominic Maggio, Yun Chang, Nathan Hughes, Matthew Trang, Dan Griffith, Carlyn Dougherty, Eric Cristofalo, Lukas Schmid, and Luca Carlone. Clío: Real-time task-driven open-set 3d scene graphs. *IEEE Robotics and Automation Letters*, 2024.
- [27] Rohit Menon, Yasmin Schmiede, Maren Bennewitz, and Hermann Blum. Open-vocabulary and semantic-aware reasoning for search and retrieval of objects in dynamic and concealed spaces. *IROS Workshop on Perception and Planning for Mobile Manipulation in Changing Environments*, 2025.
- [28] Mohammad Mohammadi, Daniel Honerkamp, Martin Büchner, Matteo Cassinelli, Tim Welschehold, Fabien Despinoy, Igor Gilitschenski, and Abhinav Valada. More: Mobile manipulation rearrangement through grounded language reasoning. In *Proc. of the IEEE/RSJ Int. Conf. on Intelligent Robots and Systems*, 2025.
- [29] Shubham Parashar, Blake Olson, Sambhav Khurana, Eric Li, Hongyi Ling, James Caverlee, and Shuiwang Ji. Inference-time computations for llm reasoning and planning: A benchmark and insights. *arXiv preprint arXiv:2502.12521*, 2025.
- [30] Sai Prasanna, Daniel Honerkamp, Kshitij Sirohi, Tim Welschehold, Wolfram Burgard, and Abhinav Valada. Perception matters: Enhancing embodied ai with uncertainty-aware semantic segmentation. *arXiv preprint arXiv:2408.02297*, 2024.
- [31] Alec Radford, Jong Wook Kim, Chris Hallacy, Aditya Ramesh, Gabriel Goh, Sandhini Agarwal, Girish Sastry, Amanda Askell, Pamela Mishkin, Jack Clark, et al. Learning transferable visual models from natural language supervision. In *Int. Conf. on Machine Learning*, pages 8748–8763, 2021.
- [32] Krishan Rana, Jesse Haviland, Sourav Garg, Jad Abou-Chakra, Ian Reid, and Niko Suenderhauf. Sayplan: Grounding large language models using 3d scene graphs for scalable robot task planning. *arXiv preprint arXiv:2307.06135*, 2023.
- [33] Zachary Ravichandran, Ignacio Hounie, Fernando Cladera, Alejandro Ribeiro, George J Pappas, and Vijay Kumar. Distilling on-device language models for robot planning with minimal human intervention. *arXiv preprint arXiv:2506.17486*, 2025.
- [34] Nils Reimers and Iryna Gurevych. Sentence-bert: Sentence embeddings using siamese bert-networks. *arXiv preprint arXiv:1908.10084*, 2019.
- [35] Antoni Rosinol, Andrew Violette, Marcus Abate, Nathan Hughes, Yun Chang, Jingnan Shi, Arjun Gupta, and Luca Carlone. Kimera: From slam to spatial perception with 3d dynamic scene graphs. *The International Journal of Robotics Research*, 40(12-14):1510–1546, 2021.
- [36] Manolis Savva, Abhishek Kadian, Oleksandr Maksymets, Yili Zhao, Erik Wijmans, Bhavana Jain, Julian Straub, Jia Liu, Vladlen Koltun, Jitendra Malik, et al. Habitat: A platform for embodied ai research. In *Proc. of the IEEE Conf. Computer Vision Pattern Recognition*, pages 9339–9347, 2019.
- [37] Fabian Schmalstieg, Daniel Honerkamp, Tim Welschehold, and Abhinav Valada. Learning long-horizon robot exploration strategies for multi-object search in continuous action spaces. In *The International Symposium of Robotics Research*, pages 52–66, 2022.
- [38] Fabian Schmalstieg, Daniel Honerkamp, Tim Welschehold, and Abhinav Valada. Learning hierarchical interactive multi-object search for mobile manipulation. *IEEE Robotics and Automation Letters*, 8(12):8549–8556, 2023.
- [39] Dhruv Shah, Michael Robert Equi, Błażej Osiński, Fei Xia, Brian Ichter, and Sergey Levine. Navigation with large language models: Semantic guesswork as a heuristic for planning. In *Conference on Robot Learning*, 2023.
- [40] Manycore Tech Inc. SpatialVerse Research Team. Interiors: A 3d gaussian splatting dataset of semantically labeled indoor scenes. <https://huggingface.co/datasets/spatialverse/InteriorGS>, 2025.
- [41] Tim Steinke, Martin Büchner, Niclas Vödisch, and Abhinav Valada. Collaborative dynamic 3d scene graphs for open-vocabulary urban scene understanding. In *IEEE/RSJ International Conference on Intelligent Robots and Systems (IROS)*, pages 6000–6007, 2025.
- [42] Andrew Szot, Alexander Clegg, Eric Undersander, Erik Wijmans, Yili Zhao, John Turner, Noah Maestre, Mustafa Mukadam, Devendra Singh Chaplot, Oleksandr Maksymets, et al. Habitat 2.0: Training home assistants to rearrange their habitat. *Advances in neural information processing systems*, 34:251–266, 2021.
- [43] Anirudh Topiwala, Pranav Inani, and Abhishek Kathpal. Frontier based exploration for autonomous robot. *arXiv preprint arXiv:1806.03581*, 2018.
- [44] Hugo Touvron, Thibaut Lavril, Gautier Izacard, Xavier Martinet, Marie-Anne Lachaux, Timothée Lacroix, Baptiste Rozière, Naman Goyal, Eric Hambro, Faisal Azhar, et al. Llama: Open and efficient foundation language models. *arXiv preprint arXiv:2302.13971*, 2023.
- [45] Abdelrhman Werby, Chenguang Huang, Martin Büchner, Abhinav Valada, and Wolfram Burgard. Hierarchical open-vocabulary 3d scene graphs for language-grounded robot navigation. In *Proc. of the Robotics: Science and Systems*,

2024.

- [46] Pengying Wu, Yao Mu, Bingxian Wu, Yi Hou, Ji Ma, Shanghang Zhang, and Chang Liu. Voronav: Voronoi-based zero-shot object navigation with large language model. *arXiv preprint arXiv:2401.02695*, 2024.
- [47] Karmesh Yadav, Ram Ramrakhya, Santhosh Kumar Ramakrishnan, Theo Gervet, John Turner, Aaron Gokaslan, Noah Maestre, Angel Xuan Chang, Dhruv Batra, Manolis Savva, et al. Habitat-matterport 3d semantics dataset. In *Proc. of the IEEE Conf. Computer Vision Pattern Recognition*, pages 4927–4936, 2023.
- [48] Hang Yin, Xiuwei Xu, Zhenyu Wu, Jie Zhou, and Jiwen Lu. Sg-nav: Online 3d scene graph prompting for llm-based zero-shot object navigation. *Advances in neural information processing systems*, 37, 2024.
- [49] Naoki Yokoyama, Sehoon Ha, Dhruv Batra, Jiuguang Wang, and Bernadette Bucher. Vlfm: Vision-language frontier maps for zero-shot semantic navigation. In *Proc. of the IEEE Int. Conf. on Robotics and Automation*, pages 42–48, 2024.
- [50] Naoki Yokoyama, Ram Ramrakhya, Abhishek Das, Dhruv Batra, and Sehoon Ha. Hm3d-ovon: A dataset and benchmark for open-vocabulary object goal navigation. in 2024 ieee. In *Proc. of the IEEE/RSJ Int. Conf. on Intelligent Robots and Systems*, pages 5543–5550, 2024.
- [51] Liding Zhang, Zeqi Li, Kuanqi Cai, Qian Huang, Zhen-shan Bing, and Alois Knoll. Language-enhanced mobile manipulation for efficient object search in indoor environments. *arXiv preprint arXiv:2508.20899*, 2025.
- [52] Mingjie Zhang, Yuheng Du, Chengkai Wu, Jinni Zhou, Zhenchao Qi, Jun Ma, and Boyu Zhou. Apexnav: An adaptive exploration strategy for zero-shot object navigation with target-centric semantic fusion. *arXiv preprint arXiv:2504.14478*, 2025.

# Relational Semantic Reasoning on 3D Scene Graphs for Open World Interactive Object Search

## - Supplementary Material -

Imen Mahdi<sup>1</sup>, Matteo Cassinelli<sup>2</sup>, Fabien Despinoy<sup>2</sup>, Tim Welschehold<sup>1</sup>, Abhinav Valada<sup>1</sup>

<sup>1</sup>University of Freiburg

<sup>2</sup>Toyota Motor Europe

### S.1. PROCEDURAL RELATIONAL SEMANTIC KNOWLEDGE DISTILLATION FOR UTILITY ESTIMATION

This section provides additional details on the procedural data generation pipeline introduced in Sec. IV-C, along with representative examples of the prompts used throughout the process.

Our objective is to construct a large and diverse open-vocabulary set of household objects. Directly prompting LLMs to generate large object lists is challenging due to token limits and their tendency to hallucinate. Moreover, repeatedly using the same prompt to generate smaller sets at each time often results in highly overlapping object sets. To address these issues, we propose a structured, multi-stage procedural generation pipeline.

For this, we use the following hierarchy:

Household  $\rightarrow$  Rooms  $\rightarrow$  Categories  $\rightarrow$  Objects

More precisely, we begin by generating a set of household room categories. Since the number of room types is relatively small, this step can be performed using a single prompt. An example of this prompt is shown in Figure S.1 (left column, top). Given the resulting set of rooms, we then generate, for each room category, a list of associated object categories using the prompt illustrated in Figure S.1 (left column, middle). Finally, for each room-object category pair, we generate a list of associated objects using the prompt shown in Figure S.1 (left column, bottom).

All generated outputs are post-processed by converting text to lowercase, enforcing space-separated words, and normalizing entries to singular nouns. This normalization avoids treating semantically identical objects as distinct due to minor formatting variations.

To further increase diversity, each prompt can be executed multiple times. The final object set is obtained by aggregating all unique outputs across runs.

Once the complete household object set is constructed, we use it to generate two relational semantic datasets: object-object co-occurrence and room-object containment. The prompts used to generate these datasets are shown in Figure S.1 (right column).

These datasets are then used to supervise the training of lightweight MLP models, as described in Sec. IV-C. An overview of the full pipeline is shown in Figure S.2.

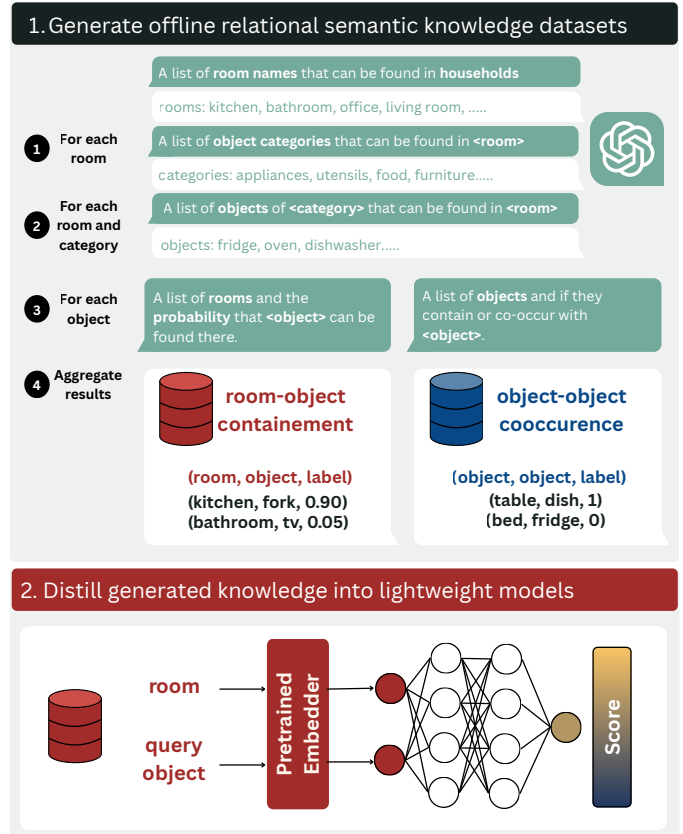


Fig. S.1: Overview of the procedural knowledge distillation pipeline. An LLM is queried procedurally to generate a diverse open-vocabulary set of household objects and relational annotations. The resulting object-object co-occurrence and room-object containment datasets are then used to supervise lightweight MLP models for utility estimation.

All data are generated using the `gpt-4o-mini` model. This model offers a trade-off between cost and performance and supports structured outputs, which simplifies parsing and reduces errors due to hallucinations or format violations.

### S.2. COMPARISON OF EMBEDDING SIMILARITY TO LEARNED RELATIONAL SEMANTIC MODELS

In Section VI-B, we evaluate the performance of our learned relational semantic models,  $f_{\theta_1}^{\text{co-occur}}$  in Eq. 3 and  $f_{\theta_2}^{\text{contain}}$  in Eq. 2, and compare them against simple embedding similarity computed using pretrained text-only embedders, including SBERT [34] and OpenAI vector embeddings, as well as the



Fig. S.2: Prompts used for procedural relational semantic knowledge distillation. Left: Prompts used to generate a large and diverse set of household objects; (top) household room categories, (middle) object categories per room, and (bottom) object set associated with each room–object category pair. Right: Prompts used to generate relational semantic datasets for object–object co-occurrence and room–object containment.

vision–language embedder CLIP [31]. For each relation type, we manually curated 100 positive and 100 negative pairs for evaluation. Table S.1 shows representative examples of the positive and negative pairs used to compare the resulting similarity scores.

To illustrate how the previously distilled relational semantic models guide exploration, we report example utility scores computed for a set of rooms and objects, along with their updated scores defined in Eq. 4. We consider multiple queries, including both in-distribution queries (highlighted in green) and

out-of-distribution queries (highlighted in yellow). Table S.9 summarizes these examples. We observe that the influence of rooms on object scores is crucial, as it allows the model to semantically differentiate objects and their uses based on their locations. For instance, cabinets and drawers are commonly found in different rooms, each typically containing specific target objects, which naturally gives them high scores. Without accounting for room context, a cabinet in the kitchen and a cabinet in the bathroom would receive the same score for a query like “dish.” By incorporating the room score, we add

TABLE S.1: Examples of positive and negative pairs used to evaluate relational semantics.

Relational Semantic	Positive Pairs		Negative Pairs	
Synonyms and Functionally Equivalent	sponge	scrubber	tv	plant
	laptop	notebook	tv	plant
	bookshelf	bookcase	broom	clock
	game console	video game system	fridge	chair
	ironing board	iron stand	fan	watch
	alarm clock	clock	bottle	car
	dresser	vanity	book	car
	heater	space heater	stove	pen
	book	novel	clock	umbrella
	soap dispenser	soap pump	tv	apple
	laundry basket	hamper	pillow	pen
	notebook	journal	table	cat
	bucket	pail	plant	clock
	conditioner	hair softener	chair	pen
	measuring cup	measuring jug	bowl	chair
	oven	cooker	toothbrush	laptop
	lamp	light	plant	headphones
	fork	utensil	painting	bottle
	can opener	tin opener	umbrella	bed
	stove	cooker	bag	lamp
Co-occur	sink	counter	controller	sink
	shower	towel	kettle	bed
	router	desk	book	toilet
	rug	couch	pillow	desk
	can opener	drawer	nightstand	microwave
	coffee table	couch	hanger	dishwasher
	remote	sofa	conditioner	rug
	vacuum cleaner	closet	eggs	rug
	toilet	bath tub	speaker	bath tub
	plate	shelf	sofa	oven
	scissors	drawer	towel rack	desk
	pan	stove	mirror	oven
	spatula	drawer	rug	toilet
	speaker	tv stand	alarm clock	toilet
	mug	table	toothpaste	coffee table
	jeans	closet	cutting board	sofa
	keyboard	desk	desk	shower
	towel rack	bath tub	microwave	bed
	microwave	oven	napkin	shower
	shoes	closet	lamp	fridge
Contain	magazine	living room	whiteboard	bathroom
	frame	living room	toothbrush	dining room
	oven	kitchen	dresser	bathroom
	drawer	bedroom	bath tub	laundry room
	toilet	bathroom	sofa	kitchen
	vacuum	laundry room	pillow	dining room
	mug	kitchen	blanket	bathroom
	laptop	office	sink	bedroom
	bookshelf	office	printer	bathroom
	sink	kitchen	knife	bedroom
	pen	office	microwave	bedroom
	book	bedroom	fork	bathroom
	mouse	office	pillow	garage
	towel rack	bathroom	bed	laundry room
	dresser	bedroom	fridge	bathroom
	table	dining room	oven	bathroom
	clothes	bedroom	pillow	bathroom
	towel	bathroom	towel rack	bedroom
	plate	kitchen	mouse	living room
	newspaper	living room	cutting board	bedroom

semantic context, reducing the score of a container if its associated room is not relevant to the target. Interestingly, because the relational models receive pretrained text embeddings as input, they generalize to descriptive queries such as ‘something to cook with’ or ‘something to sit on’, even though no similar queries are seen during training.

### S.3. 3D SCENE GRAPH DATASET EXTRACTION PIPELINE.

To create our benchmark SymSearch, we leverage the InteriorGS[40] dataset, which contains 1,000 Gaussian-splat reconstructions of human-centered indoor environments. Besides its diversity, scene complexity, and large scale, this dataset serves as an unbiased vocabulary distribution to evaluate our method on. Since the raw dataset does not provide explicit 3DSG representations, we use a semi-automated extraction pipeline, illustrated in Fig. S.3 and described in Sec. V, to create them.

## S.4. EXPERIMENTAL EVALUATIONS

### A. Implementation details

Unless stated otherwise, the agent’s hyperparameters are fixed across all experiments as follows:

TABLE S.2: Hyperparameters used to instantiate our agent in all experiments.

Hyperparameter	Value
Default room exploration score	0.7
Default frontier exploration score	0.6
$\Delta$ (utility margin)	0.1
Room influence weight $w$	0.3

For all symbolic, simulation, and real-world experiments, we used the same model checkpoints trained as described in Sec. VI-A.

### B. Baselines

1) *Embedding-Based Agents*: Existing methods leveraging embedding similarity to guide object search generally assume the agent cannot interact with the environment. They either select frontiers based on similarity scores or learn a navigation policy conditioned on embeddings. To allow for a fair comparison, we instantiate these agents identically to ours, but replace the learned approximation priors in Eq. 2 and Eq. 3 with a similarity score between the query and scene graph embeddings. Formally, the utility of a node is computed as:

$$u_q(r) \approx \text{sim}(E(q), E(r)), \quad (1)$$

for rooms, and

$$u_q(o) \approx \text{sim}(E(q), E(o)) \quad (2)$$

for objects, where  $E(\cdot)$  denotes the node embedding (from SBERT or CLIP), and  $\text{sim}(\cdot, \cdot)$  is cosine similarity.

Since the similarity distributions vary across models (see Figure 4 in the main paper), we manually tune the hyperparameters as summarized below:

TABLE S.3: Hyperparameters used for Embeddings-based agents.

Embedder	Hyperparameter	Value
SBERT	Default room exploration score	0.3
	Default frontier exploration score	0.25
	$\Delta$ (utility margin)	0.05
	Room influence weight $w$	0.3
CLIP	Default room exploration score	0.7
	Default frontier exploration score	0.4
	$\Delta$ (utility margin)	0.05
	Room influence weight $w$	0.3

TABLE S.4: Impact of room influence on embedding-based baselines. Evaluation on 200 episodes on SymSearch averaged over 5 seeds. We report Success Rate (SR), SPL, and average number of steps (N Steps).

Embedder	Room Influence	SR $\uparrow$	SPL $\uparrow$	N Steps $\downarrow$
CLIP	$\times$	$0.562 \pm 0.021$	$0.177 \pm 0.012$	$38 \pm 1$
	$\checkmark$	$0.638 \pm 0.013$	$0.171 \pm 0.020$	$34 \pm 1$
SBERT	$\times$	$0.598 \pm 0.010$	$0.173 \pm 0.024$	$38 \pm 1$
	$\checkmark$	$0.683 \pm 0.019$	$0.179 \pm 0.024$	$33 \pm 1$

We also compare two variants of the embedding-based baselines, with and without room influence, to highlight their impact on performance. Results on **SymSearch** are summarized in Table S.4. We show that adding the room context improves the overall success rate even when estimated utility scores are noisy.

2) *LLM-Based Agents*: We compare our method against two approaches that use online LLM planners for interactive object search. Both methods share the same pipeline as our agent—namely, constructing a 3D scene graph (3DSG) from raw observations and mapping high-level actions to low-level policies—and differ only in how the next node to explore is selected. We describe each approach below.

a) *MoMaLLM*: We follow the prompt format proposed in the original work [18]. An example prompt is shown in Figure S.4. To reduce hallucinations, we use structured outputs that constrain the model to select only valid actions and arguments. The LLM is additionally provided with a history of the previous 30 actions and their outcomes to discourage repeatedly selecting the same actions.

b) *GODHS*: GODHS [51] uses a different approach that significantly reduces the number of LLM calls performed during online exploration. The agent first explores all rooms and frontiers in the environment. It then queries the LLM to rank the visited rooms according to their relevance to the target object (Figure S.5) and visits them in this order. Within each room, the LLM is first asked to identify potential carriers for the target object (Figure S.6) and then to rank these carriers by the likelihood of containing the queried object (Figure S.7). While this approach improves runtime efficiency by limiting repeated LLM calls, it introduces an additional exploration phase.

c) *LLM Variant Selection*: We preselect the LLM model and variant for these baselines by evaluating the performance of MoMaLLM on 50 sample episodes from SymSearch. Our goal is to choose the best model variant that balances success

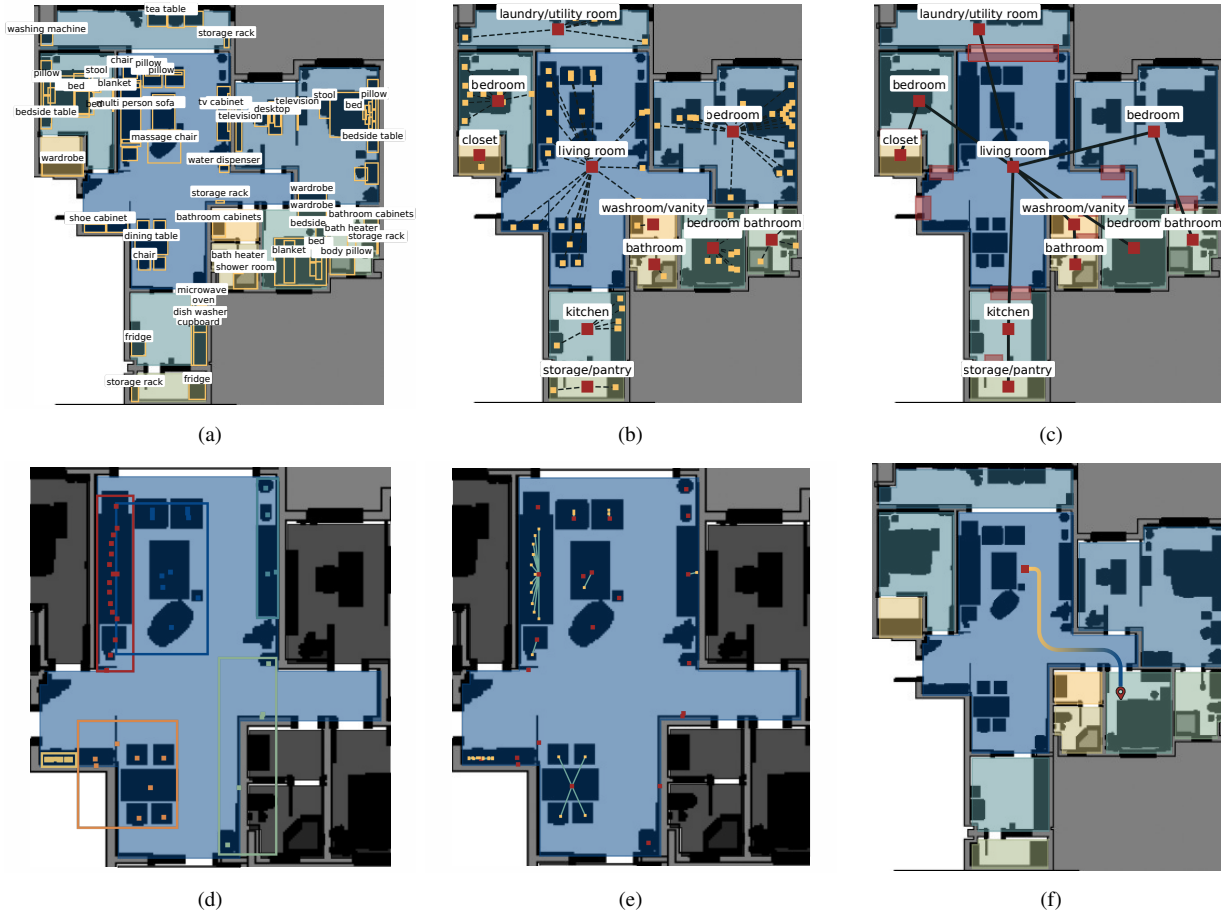


Fig. S.3: **3DSG construction pipeline from InteriorGS scenes.** (a) Each scene includes a top-down occupancy map, annotated object bounding boxes, room polygons, and door/opening bounding boxes, which we use to construct the 3DSG. (b) Each object’s position is defined as the center of its bounding box. Objects are assigned to rooms if their centers lie within the corresponding room polygon. Rooms are annotated using an LLM based on their contents, and are then manually verified for consistency. (c) To determine room connectivity, door polygons are dilated, and rooms sharing an intersecting door are marked as connected. (d) To define spatially coherent regions within rooms, we cluster object  $(x, y)$  coordinates using a Gaussian Mixture Model. Each cluster represents a distinct region. (e) Nested object relationships (e.g., *on-top-of*, *inside*) are manually annotated by experts by inspecting the Gaussian splats. (f) Traveled distances are computed by first identifying the closest unoccupied pixel to the goal object within the same room on a dilated occupancy map, then applying A\* to compute realistic geodesic paths from the agent to the goal.

rate, inference time, and cost. All models were evaluated under similar runtime conditions: local models on an NVIDIA GeForce RTX 4060 Ti, and the others under comparable network settings. The results are summarized in Table S.5.

Mistral [20] and LLaMA [44] are open-source models that can be run locally and have relatively small sizes (7B and 8B parameters, respectively). However, both perform poorly in this setting. In particular, Mistral frequently fails to follow instructions and often produces invalid outputs. LLaMA is more reliable in producing parseable responses but appears to lack the common-sense reasoning required to perform the task efficiently.

In contrast, the proprietary models from DeepSeek [14], Claude [3], and OpenAI [1] consistently exhibit stronger common-sense behavior and achieve higher success rates. While deepseek-reasoner achieves the highest success rate, its additional thinking mode significantly increases inference time, which limits large-scale evaluations. While deepseek-chat runs faster, it suffers from lower perfor-

mance. Both claude-sonnet-4-5 and gpt-4o perform well and are relatively fast, but are significantly more expensive. Overall, we find gpt-5-mini to provide the best trade-off between performance, runtime, and cost, and use it for all LLM-based experiments.

### C. Benchmarks

In this section, we provide more details and examples of the evaluation benchmarks we used in Sec. VI.

1) *SymSearch*: We select 10 scenes from the InteriorGS dataset and define 200 episodes, with examples provided in Table S.7. Each episode specifies a query object located within one of the annotated scenes. To simulate interactive search, we assume that all nested objects are either inside or on top of another object, requiring the agent to explore the parent object to locate them. For non-interactive scenarios, we assume the target object is visible upon exploring the room in which it is located.

TABLE S.5: **Comparison of LLM variants for interactive object search.** We report model specifications and performance metrics on SymSearch. Prices are reported per 1 million tokens (Input / Output).

Model Card						Performance			
Model	Version	Pricing (Input / Output)	Size	Local	Structured Output	SR ↑	SPL ↑	Steps ↓	Inference Time (s) ↓
Mistral	Mistral-7B-Instruct-v0.1	Open-source	7B	✓	×	0.24	0.149	42	146
LLaMA	Meta-Llama-3.1-8B-Instruct	Open-source	8B	✓	×	0.24	0.139	39	423
DeepSeek	deepseek-chat	\$0.028 / \$0.42	671B	×	×	0.78	0.222	24	44
	deepseek-reasoner			×	×	0.96	0.356	15	721
Claude	claude-sonnet-4-5	\$3 / \$15	Undisclosed	×	✓	0.82	0.216	23	171
GPT	gpt-3.5-turbo	\$3 / \$6	Undisclosed	×	×	0.50	0.179	33	23
	gpt-4o-mini	\$0.15 / \$0.60		×	✓	0.68	0.172	27	117
	gpt-4o	\$2.5 / \$10		×	✓	0.80	0.293	20	116
	gpt-5-mini	\$0.25 / \$2		×	✓	0.88	0.304	19	278

**Prompt used for MoMa-LLM**

You are a robot with a manipulator arm in an unexplored house. Your task is to locate **storage basket**. You have the following actions available that you can use to achieve this task:

- navigate\_to(room\_id)**: navigate to this room.
- go\_to\_and\_search(room\_id, object\_id)**: go to this object or container and explore around it, on top of it, under it, and inside of it.
- explore\_frontier(room\_id)**: explore the unknown space inside this room that is not fully explored yet.
- explore\_unknown\_room(room\_id)**: explore the unknown room.
- done!**: call when the task is completed or if you are unable to take any further actions.

You must respond with three items, Analysis, Reasoning, and Command, as below:

**Reasoning**: describe where you could find the objects of interest and what actions you need to execute to get there.

**Command**: function call, name of the function to call. Example "go\_to\_and\_search" has to be one of the given options.

**Args**: A list of (arg, value) pairs to pass to the function as arg=value. Has to respect the format of the command chosen.

**Current Scene Description**:  
 You are currently in room-8. You are standing next to the following objects: [object-351(storage rack)]. Furthermore, you have found the following rooms and objects in the house so far given in format: room\_id(room\_label): [object\_id(object\_label),...]

- room-8(bathroom): [object-460(shower head),object-351(storage rack)]
- room-9(corridor): []

These rooms are unexplored: [unexplored\_room-2, 'unexplored\_room-4', 'unexplored\_room-0'].  
 These rooms have unexplored frontiers within the room: {room-8}.

Your 30 previous actions were: [explore\_unknown\_room(room\_id=unexplored\_room-8) - succeeded], explore\_frontier(room\_id=room-8) - succeeded]

What is the best next action to complete the task as efficiently as possible?  
 Remember:

- You can only use the objects and rooms that you have already found. Object ids and room ids have to match the description exactly.
- You can only explore rooms that are listed as having unexplored space.
- Explore all areas that might contain relevant objects before calling done!.
- If you have fully completed the task, directly call done!.

**Reasoning**:  
 I am already next to object-351 (storage rack) in room-8, so using go\_to\_and\_search on that object is the quickest way to determine if the storage basket is present. This avoids unnecessary travel to other rooms and respects the requirement to explore nearby candidate containers before moving on.

**Parsed Command**:  
 go\_to\_and\_search(room\_id='room-8', object\_id='object-351')

Fig. S.4: **Prompt used for the MoMaLLM baseline.** The agent is given a precise description of the scene and a history of previous actions taken. The agent selects the best action to take next and grounds it to the identified scene elements.

2) *OmniGibson*: We extend OmniGibson with an interactive object search task definition. We leverage the simulator’s internal instance sampler and the large set of objects from the Behavior1K [22] dataset. Each episode is defined by the object category, an optional parent object and predicate, and optionally the room in which the object should be spawned.

If a parent object is specified, we first check whether it exists in the target room (or elsewhere in the scene if no room is specified). If it does not exist, we sample the parent object in the scene before sampling the target object according to the

**Prompts Used For GODHS: Rank Room**

You are an agent in a household, your task is to look for **teapot**. The household contains the following rooms and their categories in the format - 'room\_id': 'room\_type':

- room-0 : living room/kitchen
- room-1 : master bedroom
- room-2 : bedroom
- room-3 : bathroom
- room-4 : toilet
- room-5 : bedroom.

**Order the rooms in likelihood probability that the room would contain a teapot. Return a list of room\_ids.**

**Rooms Ranked**:  
 [room-0, 'room-1', 'room-2', 'room-5', 'room-3', 'room-4']

---

**Prompts Used For GODHS: Identify Carriers**

You are an agent in a household in the room **living room/kitchen**, your task is to look for **teapot**. The household contains the following objects and their categories in the format - 'object\_id': 'object\_type':

- object-97 : cabinet
- object-137 : chair
- object-92 : wardrobe
- object-135 : dining table
- object-136 : chair
- ...
- object-322 : chopping board
- object-326 : storage rack
- object-234 : refrigerator
- object-324 : kitchen supplies combination
- object-121 : teatable

**You need to identify possible carriers for teapot. A carrier is an object in the room that can contain teapot either on top, under, on the sides, or inside of it. Return a list of only object\_ids that can carry teapot, and remove all irrelevant objects from the list.**

**Possible Carriers**:  
 [object-97, 'object-92', 'object-135', 'object-121', 'object-117', 'object-285', 'object-322', 'object-325', 'object-326', 'object-324', 'object-234', 'object-140', 'object-137', 'object-136', 'object-139', 'object-138', 'object-116', 'object-118', 'object-111']

Fig. S.5: **GODHS prompt for ranking rooms.** The LLM ranks all visited rooms based on their relevance to the target object.

Fig. S.6: **GODHS prompt for identifying carriers.** The LLM selects potential carriers within a room that may contain the target object.

specified predicate. If no parent object is specified, we first check whether the target object exists in the room; if it does, we use it as the target, otherwise, we sample it in that room. If no room is specified, we select any instance of the target category in the scene or randomly sample one if none exists.

Success is defined as the agent having the target object visible and within a distance threshold. Table S.6 provides descriptions of all evaluation episodes, including all unique object categories used in our experiments.

```
Prompts Used For GODHS: Sort Carriers

You are an agent in a household in the room living room/kitchen, your task is to look for teapot.
The following carriers are identified as possible locations to check. They are given as:
- 'carrier_id': 'carrier_type'

- object-97 : cabinet
- object-137 : chair
- object-92 : wardrobe
- object-135 : dining table
...
- object-234 : refrigerator
- object-121 : teatable
- object-118 : armchair
- object-138 : chair
- object-117 : teatable

Order these carriers in likelihood probability that the carrier would contain a teapot either on top, under, next to, or
inside of it. Return a list of carrier_ids in search order. If none apply or no objects found, return an empty list.

Carriers Sorted:
[object-121, 'object-117', 'object-135', 'object-97', 'object-324', 'object-325', 'object-326', 'object-285', 'object-140', 'object-
322', 'object-234', 'object-92', 'object-116', 'object-118', 'object-137', 'object-136', 'object-139', 'object-138', 'object-111']
```

Fig. S.7: **GODHS prompt for sorting carriers**. The LLM ranks the identified carriers by likelihood of containing the target object.

#### D. Real World Experiments

We deploy our method on a real robot manipulator as described in Sec. VI-E. In Table S.8, we provide descriptions of each evaluation setup along with their outcomes.

TABLE S.6: Examples of evaluation episodes from OmniGibson

Query	Scene	Interactive	Location Description
chopstick	Pomaria_1_int	×	on top of a breakfast_table in a kitchen
wall_mounted_tv	Wainscott_0_int	×	on top of a console_table in a living_room
lipstick	Beechwood_0_int	×	on top of a sink in a bathroom
vacuum	Beechwood_0_int	×	in a utility_room
keyboard	Beechwood_0_int	×	on top of a desk in a private_office
dental_floss	Merom_0_int	✓	inside of a bottom_cabinet in a bathroom
pants	Beechwood_1_int	✓	inside of a hamper in a bedroom
box_of_sanitary_napkins	Beechwood_1_int	✓	inside of a top_cabinet in a bathroom
measuring_cup	Merom_1_int	✓	inside of a bottom_cabinet in a kitchen
espresso_machine	Pomaria_1_int	×	on top of a countertop in a kitchen
wooden_spoon	Wainscott_0_int	✓	inside of a bottom_cabinet in a kitchen
toy_box	Beechwood_1_int	×	in a childs_room
chopping_board	Beechwood_0_int	×	on top of a countertop in a kitchen
pen	Beechwood_0_int	✓	inside of a bottom_cabinet in a private_office
water_bottle	Beechwood_0_int	×	on top of a coffee_table in a living_room
colored_pencil	Beechwood_0_int	×	on top of a desk in a private_office
lunch_box	Beechwood_0_int	✓	inside of a fridge in a kitchen
paper_sheet	Beechwood_0_int	✓	inside of a bottom_cabinet in a private_office
magazine	Beechwood_1_int	✓	inside of a bookcase
video_game	Wainscott_0_int	×	on top of a console_table
box_of_shampoo	Merom_0_int	×	in a bathroom
plate	Pomaria_1_int	✓	inside of a microwave
charger	Wainscott_1_int	×	on top of a desk
can_of_soda	Pomaria_1_int	✓	inside of a fridge in a kitchen
soap_dispenser	Merom_0_int	×	on top of a sink
blanket	Pomaria_2_int	×	on top of a armchair
deodorant_stick	Beechwood_1_int	✓	inside of a top_cabinet in a bathroom
box_of_milk	Rs_garden	✓	inside of a fridge in a kitchen
canned_food	Rs_garden	✓	inside of a bottom_cabinet in a kitchen
toothbrush	Rs_garden	×	on top of a sink in a bathroom
wineglass	Beechwood_0_int	✓	inside of a top_cabinet in a kitchen
detergent_bottle	Beechwood_0_int	✓	inside of a bottom_cabinet in a utility_room
laptop	Beechwood_0_int	×	on top of a desk in a private_office
toy_figure	Beechwood_1_int	✓	inside of a bottom_cabinet in a childs_room
plate	Beechwood_0_int	×	on top of a coffee_table in a dining_room
teacup	Beechwood_0_int	×	on top of a coffee_table in a living_room
newspaper	Merom_0_garden	×	on top of a coffee_table in a garden
frying_pan	Wainscott_0_int	×	on top of a stove in a kitchen
pants	Ihlen_0_int	✓	inside of a clothes_dryer in a storage_room
coffee_maker	Wainscott_0_int	×	in a kitchen
sponge	Wainscott_0_int	×	on top of a sink
bowl	Wainscott_0_int	✓	inside of a dishwasher in a kitchen
clipper	Rs_garden	✓	inside of a bottom_cabinet in a bedroom
bottle_of_soy_sauce	Pomaria_1_int	×	on top of a countertop in a kitchen
yogurt_carton	Pomaria_1_int	✓	inside of a fridge in a kitchen
club_sandwich	Pomaria_1_int	✓	inside of a fridge in a kitchen
notepad	Wainscott_1_int	×	on top of a desk in a private_office
paperback_book	Beechwood_1_int	✓	inside of a bookcase
carving_knife	Beechwood_0_int	✓	inside of a dishwasher in a kitchen
tank_top	Ihlen_0_int	✓	inside of a washer in a storage_room

TABLE S.7: Examples of evaluation episodes from SymSearch

Query	Scene	Interactive	Location Description
teapot	0900	✓	on top of a teatable in a combined living room and kitchen
fruit	0900	✓	on top of a chopping board in a combined living room and kitchen
refrigerator	0900	×	in a combined living room and kitchen
armchair	0900	×	in a combined living room and kitchen
bed	0900	×	in a master bedroom
toilet	0900	×	in a toilet
book	0901	✓	inside a wardrobe in a bedroom
blanket	0901	✓	on top of a bed in a bedroom
knife	0901	✓	inside a chopping board in a kitchen
vegetable	0901	✓	on top of a chopping board in a kitchen
eggbeater	0902	✓	inside a cabinet in a kitchen
spatula	0902	✓	inside a cabinet in a kitchen
towel	0902	✓	inside a storage rack in a kitchen
spoon	0902	✓	inside a storage rack in a kitchen
clothes hanger	0902	✓	inside a wardrobe in a bedroom
tv	0902	×	in a bedroom
cat tower	0902	×	in a living room
multi person sofa	0902	×	in a living room
flowers	0904	✓	on top of a side table in a living room
chair	0904	✓	on top of a dining table in a living room
shoe	0904	✓	inside a shoe cabinet in a living room
television	0904	✓	on top of a tv cabinet in a living room
notebook computer	0904	✓	on top of a tea table in a living room
keyboard	0904	✓	on top of a table in a bedroom
mouse	0904	✓	on top of a table in a bedroom
bowl	0904	✓	inside a cupboard in a kitchen
dish	0904	✓	inside a cupboard in a kitchen
tissue	0904	✓	inside a toilet paper holder in a bathroom
side table	0904	×	in a living room
clock	0904	×	in a living room
fan	0904	×	in a living room
water dispenser	0904	×	in a living room
tv cabinet	0904	×	in a living room
massage chair	0904	×	in a living room
tea table	0904	×	in a living room
trash can	0904	×	in a living room
bookshelf	0904	×	in a bedroom
oven	0904	×	in a kitchen
electric cooker	0904	×	in a kitchen
microwave	0904	×	in a kitchen
cupboard	0904	×	in a kitchen
bracelet	0906	✓	inside a cabinet in a bedroom (master)
glasses	0906	✓	inside a cabinet in a bedroom (master)
chopsticks	0906	✓	inside a storage rack in a kitchen
faucet	0906	✓	on top of a washing station in a bathroom
table lamp	0906	×	in a combined living and dining room
display cabinet	0906	×	in a combined living and dining room
toy bus	0906	×	in a bedroom
eggbeater	0906	×	in a kitchen
balance	0906	×	in a bedroom (master)
red wine glass	0908	✓	on top of a dining table in a combined living and dining room
candy	0908	✓	inside a bowl in a combined living and dining room
headphones	0908	✓	inside a display cabinet in a combined study and library
notebook	0908	✓	inside a storage rack in a bedroom
rice cooker	0909	✓	inside a storage rack in a kitchen

TABLE S.8: Results on real world experiments.

Query	Interactive	Location Description	Outcome
milk bottle	✓	inside the fridge in the kitchen	Success Success Perception Failure
remote-controller	×	on top of the table in the living room	Success Success Perception Failure
book	✓	inside the bookshelf in the living room	Success Success Manipulation Failure
blanket	×	on top of the sofa in the living room	Success Success Success
spatula	✓	inside the drawer in the kitchen	Success Success Success
plate	✓	inside the cabinet in the kitchen	Success Manipulation Failure Perception Failure
keyboard	×	on top of the desk in the office	Success Success Success
teddy-bear	×	on top of the sofa in the living room	Success Success Perception Failure
pen	✓	inside the fridge in the kitchen	Success Success Perception Failure
fruit	✓	inside the fridge in the kitchen	Success Success Reasoning Failure
cup	×	inside the fridge in the kitchen	Success Success Perception Failure
monitor	×	inside the fridge in the kitchen	Success Perception Failure Reasoning Failure

TABLE S.9: Example utility scores for room and objects categories across multiple queries. In-distribution queries are highlighted in green, out-of-distribution queries in yellow, and descriptive queries in blue.

Query	Room Type	Room Score	Object	Object Score	Updated Score
plate	kitchen	0.78	cabinet	0.94	0.75
			counter	0.99	0.78
			sink	0.94	0.75
			table	0.92	0.74
			fridge	0.45	0.48
			chair	0.12	0.30
	living room	0.30	sofa	0.00	0.09
			cabinet	0.94	0.29
			coffee table	0.82	0.26
	bathroom	0.21	tv	0.04	0.10
			sink	0.94	0.20
			cabinet	0.94	0.20
	bedroom	0.20	bathtub	0.00	0.06
			bed	0.00	0.06
			cabinet	0.94	0.20
		wardrobe	0.08	0.07	
		nightstand	0.31	0.11	
toothpaste	bathroom	0.88	cabinet	1.00	0.88
			sink	0.99	0.88
			bathtub	0.19	0.39
	bedroom	0.55	cabinet	1.00	0.55
			nightstand	0.99	0.55
			wardrobe	0.48	0.35
			bed	0.01	0.17
	kitchen	0.36	cabinet	1.00	0.36
			sink	0.99	0.36
			table	0.88	0.33
			fridge	0.10	0.13
			chair	0.00	0.11
lip gloss	bathroom	0.65	sink	0.83	0.58
			cabinet	0.99	0.65
			bathtub	0.00	0.20
	bedroom	0.58	nightstand	0.99	0.58
			cabinet	0.99	0.58
			wardrobe	0.28	0.29
	kitchen	0.37	counter	1.00	0.37
			cabinet	0.99	0.37
melon	kitchen	0.97	fridge	0.03	0.12
			counter	0.99	0.97
			cabinet	0.92	0.92
			table	0.73	0.79
			fridge	0.33	0.51
	living room	0.42	sink	0.09	0.35
			coffee table	0.73	0.34
	bathroom	0.17	sofa	0.00	0.13
			cabinet	0.92	0.16
			sink	0.09	0.06

Query	Room Type	Room Score	Object	Object Score	Updated Score
a brown leather jacket	bedroom	0.80	wardrobe	0.99	0.79
			nightstand	0.92	0.75
			cabinet	0.87	0.72
			bed	0.07	0.28
	living room	0.72	cabinet	0.87	0.66
			coffee table	0.42	0.43
			tv	0.01	0.22
			sofa	0.01	0.22
	bathroom	0.10	cabinet	0.87	0.09
			bathtub	0.00	0.03
a snack to eat	kitchen	0.62	counter	1.00	0.62
			table	0.96	0.60
			cabinet	0.96	0.60
			fridge	0.80	0.53
			sink	0.01	0.19
	living room	0.53	coffee table	0.98	0.52
			sofa	0.00	0.16
			tv	0.00	0.16
	bathroom	0.09	cabinet	0.96	0.51
			cabinet	0.96	0.09
			sink	0.01	0.03
			bathtub	0.00	0.03